Molecular State Reconstruction by Nonlinear Wave Packet Interferometry

Travis S. Humble and Jeffrey A. Cina*

Department of Chemistry and Oregon Center for Optics, University of Oregon, Eugene, Oregon 97403, USA

(Received 17 November 2003; published 6 August 2004)

We show that time- and phase-resolved two-color nonlinear wave packet interferometry can be used to reconstruct the probability amplitude of an optically prepared molecular wave packet without prior knowledge of the underlying potential surface. We analyze state reconstruction in pure- and mixed-state model systems excited by shaped laser pulses and propose nonlinear wave packet interferometry as a tool for identifying optimized wave packets in coherent control experiments.

DOI: 10.1103/PhysRevLett.93.060402 PACS numbers: 03.65.Wj, 33.80.–b, 42.50.Md, 42.87.Bg

Several groups have demonstrated that adaptive laser control can influence a variety of photochemical processes [1–4]. Those experiments determine the optical waveform needed to drive a chemical reaction to a desired product. But optimization of an incident waveform neither directly elucidates the light-induced reaction mechanism nor identifies the optically prepared initiating state, especially if the relevant electronic potential energy surface(s) are ill characterized. Therefore, methods for directly determining an optically prepared molecular state are being sought [5–9]. Here we propose reconstruction by two-color nonlinear wave packet interferometry (WPI) as a means for determining an initial dynamical state in which detailed prior knowledge of the excited-state Hamiltonian is not required.

Linear WPI [10,11] measures the interference contribution to an excited-state population arising from the overlap between nuclear wave packets prepared by a phase-locked pulse pair. By shifting the optical phase difference, the real and imaginary components of the overlap are isolated. State reconstruction by linear WPI has been suggested as a form of quantum state holography (QSH) [7,8]. In QSH, one isolates the complex overlap between shaped target and short-pulse reference wave packets and reconstructs the target by inverting a set of linear algebraic equations.

Nonlinear WPI [9,12] is more powerful than its linear realization in several respects. This heterodyne-detected interference spectroscopy [13,14] employs a *pair* of phase-locked *pulse pairs* to create an excited-state population quadrilinear in the electric field amplitudes. In the two-color case, the first pulse pair accesses an intermediate electronic state (e), while the second transfers amplitude from the ground state (g) to a final state (f). Overlaps between a shaped target wave packet launched in the f state by the third pulse and a family of variable reference wave packets prepared in f via the g and e states through the combined action of the first, second, and fourth pulses can be measured by combining signals taken with different phase-locking angles. In the short-pulse limit, the reference states are faithfully copied to the final surface regardless of its spatial form, and the isolable overlaps enable determination of the target state probability amplitude (as opposed to the probability density [5,6]) without detailed knowledge of that surface. This feature contrasts with other forms of molecular state reconstruction [5–8].

We consider the nuclear Hamiltonians H_g and H_e to be known, while the f-state Hamiltonian H_f need not be. The electronic transition dipoles μ_{eg}, μ_{fe}, and μ_{fg} are independent of nuclear coordinates (Condon approximation) and are here taken parallel with the polarization of the electric field. The latter comprises four pulses, which have arrival times t_j ($t_1 < t_2 < t_3 < t_4$), envelopes $A_j(t)$, and phases $\Phi_j(t)$. In the slowly varying envelope approximation, the Fourier component of the jth field at $\omega > 0$ has spectral amplitude $\alpha_j(\omega)$ and phase $\phi_j(\omega) - \omega t_j$. The first pulse pair drives $e \leftrightarrow g$ and is phase locked at ω_L with locking angle $\phi_{21} = \phi_2(\omega_L) - \phi_1(\omega_L) - \omega_L t_{21}$, ($t_{ij} = t_i - t_j$), while the second pulse pair drives $f \leftarrow g$ and is phase locked at ω_L' with angle $\phi_{43} = \phi_4(\omega_L') - \phi_3(\omega_L') - \omega_L' t_{43}$.

For $t \ll t_1$, the molecular state is $|\Psi(t)\rangle = |g\rangle \times \exp[-iH_g(t - t_3)]|\gamma\rangle$, where $|\gamma\rangle$ is a g-state vibrational eigenstate and $\hbar = 1$. Following the last pulse, the final-state amplitude linear and trilinear in the weak electric fields is a superposition of four wave packets [15]; two wave packets result from the first-order action of pulses 3 and 4, while another two result from the sequential action of pulses 1, 2, and 3 or 4. The nonlinear WPI signal is the f-state population quadrilinear in the fields:

$$S(\phi_{21}, \phi_{43}) = 2\,\mathrm{Re}[\langle \mathrm{ref}_{421}|\mathrm{tar}_3\rangle e^{-i(\phi_{21}-\phi_{43})} + \langle \mathrm{ref}_{321}|\mathrm{tar}_4\rangle e^{-i(\phi_{21}+\phi_{43})}]. \quad (1)$$

The complex quantities $\langle \mathrm{ref}_{421}|\mathrm{tar}_3\rangle$ and $\langle \mathrm{ref}_{321}|\mathrm{tar}_4\rangle$ are independent of the phase-locking angles and can be isolated by combining signals with different optical phase shifts [10,16]:

 © 2004 The American Physical Society

$$\langle \mathrm{ref}_{421}|\mathrm{tar}_3\rangle = \frac{1}{4}\left[S(0,0) + S\left(\frac{\pi}{2},\frac{\pi}{2}\right)\right] + \frac{i}{4}\left[S\left(\frac{\pi}{2},0\right) + S\left(0,-\frac{\pi}{2}\right)\right], \quad (2)$$

$$\langle \mathrm{ref}_{321}|\mathrm{tar}_4\rangle = \frac{1}{4}\left[S(0,0) - S\left(\frac{\pi}{2},\frac{\pi}{2}\right)\right] + \frac{i}{4}\left[S\left(\frac{\pi}{2},0\right) - S\left(0,-\frac{\pi}{2}\right)\right]. \quad (3)$$

Both isolated components are overlaps between a one-pulse *target* state and a three-pulse *reference* state. The overlap (3) is between a nearly momentumless target state prepared in f by the fourth pulse and a reference that propagates in all three electronic levels. Of greater interest here is the overlap (2) between the target,

$$|\mathrm{tar}_3\rangle = e^{-iH_f t_{43}} P_3^{fg} |\gamma\rangle e^{i\phi_3(\omega_L') + i\omega_L' t_{43}}, \quad (4)$$

generated by the third pulse and propagated for time t_{43} in the f state, and a reference,

$$|\mathrm{ref}_{421}\rangle = -P_4^{fg} e^{-iH_g t_{42}} P_2^{eg\dagger} e^{-iH_e t_{21}} P_1^{eg} e^{iH_g t_{31}} |\gamma\rangle e^{i\phi_4(\omega_L') - i\phi_{21}}, \quad (5)$$

which propagates only in g and e. The pulse propagator,

$$P_j^{ab} = i\frac{\mu_{ab}}{2}\int_{-\infty}^{\infty} dt\, A_j(t) e^{-i\Phi_j(t)} e^{iH_a t} e^{-iH_b t}, \quad (6)$$

transfers nuclear amplitude from electronic state b to the higher-lying state a, while $P_j^{ab\dagger}$ governs the reverse transition. In scans of fixed t_{43} and varying (t_{21}, t_{32}), measurements of $\langle \mathrm{ref}_{421}|\mathrm{tar}_3\rangle$ provide amplitude-level information on the target wave packet in terms of well-characterized reference states [17]. Reconstruction of the target can then be performed by inverting the resulting set of linear algebraic equations by singular value decomposition (SVD) [18].

To test our reconstruction procedure, we calculated the nonlinear WPI signal for a one-dimensional system comprising harmonic g and e states and a dissociative f state. The f-state potential is $V_f(x) = De^{-ax} + \varepsilon_f$ with $D = 2\pi c$ (1000 cm^{-1}) and $a = 9.124$ Å^{-1}. Both harmonic potentials have frequency $\omega = 2\pi c$ (210 cm^{-1}) and reduced mass $m = 63.5$ amu, with the e-state minimum ε_e displaced by $x_e = 0.0614$ Å relative to the g state [19]. We take $\Phi_j(t) = \Phi_j + \Omega_j t + c_j t^2/2$ and $A_j(t) = E_j' \exp[-t^2/2\sigma_j'^2]$, with (uncontrolled) absolute phase Φ_j, carrier frequency Ω_j, temporal chirp rate c_j, peak amplitude E_j', and pulse width σ_j' [20]. The interferogram (2) was calculated for a system initially in the ground vibrational state using grid-based propagation techniques for time evolution under the nuclear Hamiltonians and split propagators to evaluate the pulse propagators (6) in the position representation [21]. Delays t_{21} and t_{32} were scanned over one vibrational period, $\tau_g = 158.8$ fs, in 3.17-fs steps and the target-defining delay $t_{43} = 25.4$ fs. T was varied to maximize the fidelity [18].

We first consider the target state prepared by a transform-limited third pulse. Using the interferogram shown in Fig. 1, with the addition of Gaussian random noise (standard deviation 5% of signal maximum), the target wave packet is reconstructed with fidelity 0.988 ($T = 0.0137$). The deviation from unity results mainly from the absence of reference amplitude far from the Franck-Condon point, where the difference between the g and the f potentials is in the red wing of the pulse bandwidth [22].

To explore reconstruction of optically shaped target states, we use a chirped third pulse. The target states for the cases of maximal positive and negative temporal chirp are shown in Fig. 2. The collection of delay-dependent reference states is the same in both cases; differences in the interferograms (not shown) result en-

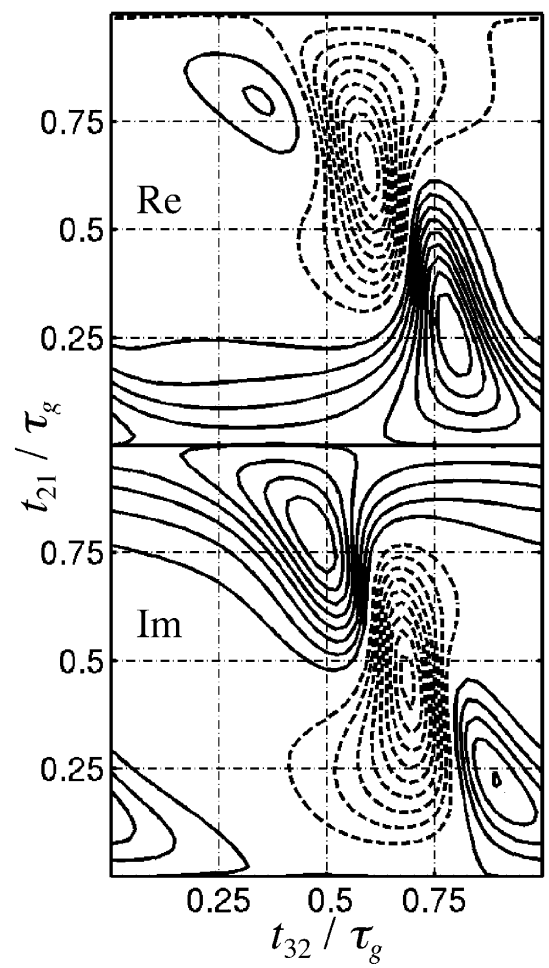

FIG. 1. Real and imaginary components of the interferogram (2) with all four pulses transform limited. Solid (dashed) contours represent regions of positive (negative) interference.

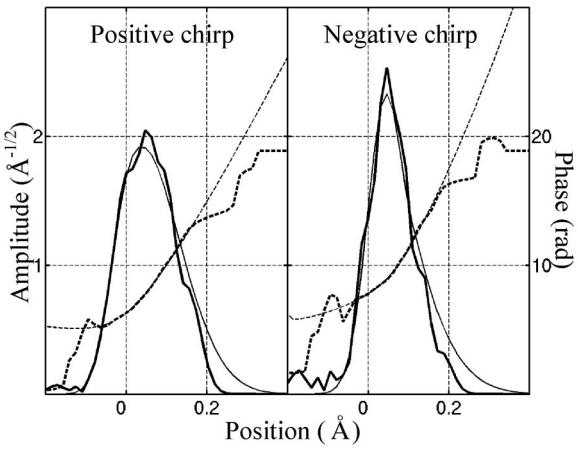

FIG. 2. Amplitude (solid line) and phase (dashed line) of target (fine line) and reconstructed (heavy line) wave packets from positively and negatively chirped pulses.

tirely from the different target states (which have a mutual normalized overlap of 0.942). With addition of 5% noise to the signals, the reconstructed states in Fig. 2 have fidelities 0.984 and 0.979, respectively ($T = 0.0137$). Accurate reconstruction in the presence of noise is a consequence of preparing many overlapping reference states (analogous to overcomplete coherent states), so that the nonlinear WPI signal contains highly redundant information.

These examples of reconstruction have implicitly utilized knowledge of the f-state Hamiltonian via P_4^{fg}. We may also investigate reconstruction when no such information is available, and the fourth pulse is treated as impulsive despite its nonzero duration [23]. The rows of the reference matrix then contain scaled copies of the ground-state wave packets prepared by pulses 1 and 2. Using this reference matrix and the rigorously calculated signal from Fig. 1 with 5% noise, the target state was reconstructed with fidelity 0.985 ($T = 0.0258$). The loss in fidelity is due to the approximate reference states' exaggerated amplitude in spatial regions far from the resonance point of the fourth pulse. In the absence of f-state information, accurate reconstruction of an arbitrary target state requires an ultrashort fourth pulse, with spectral amplitude spanning the potential difference throughout the region where the target state is localized.

Our reconstruction procedure can be extended to systems with initial equilibrium mixed-state density matrices $\rho = \sum w_\gamma |\gamma\rangle\langle\gamma|$, where w_γ is the population of level γ. The nonlinear WPI signal is the weighted sum

$$S(\phi_{21}, \phi_{43}) = 2\,\mathrm{Re} \sum w_\gamma (\langle \mathrm{ref}_{421}^\gamma | \mathrm{tar}_3^\gamma \rangle e^{-i(\phi_{21}-\phi_{43})} + \langle \mathrm{ref}_{321}^\gamma | \mathrm{tar}_4^\gamma \rangle e^{-i(\phi_{21}+\phi_{43})}), \quad (7)$$

where the superscript denotes the state from which the target and reference wave packets originate. Reconstruction proceeds as in the pure state case [24] but with a cumulative fidelity $f = \sum w_\gamma f_\gamma$.

To illustrate mixed-state reconstruction, we use our previously described model system with thermally populated g-state vibrational levels. At 298 K, we include the first five levels, accounting for 99.4% of the total population. Figure 3 (left panels) shows the target wave packets prepared from the lowest three levels by a transform-limited third pulse. States reconstructed from the calculated signal with 5% noise are shown in Fig. 3 (right panels). The individual fidelities in ascending state order are 0.979, 0.942, 0.837, 0.594, and 0.476 ($T = 0.0185$). Reconstruction of those targets with initial population below the noise level is poor. The cumulative fidelity is 0.935.

State reconstruction by nonlinear WPI could serve as a diagnostic tool for identifying target wave packets

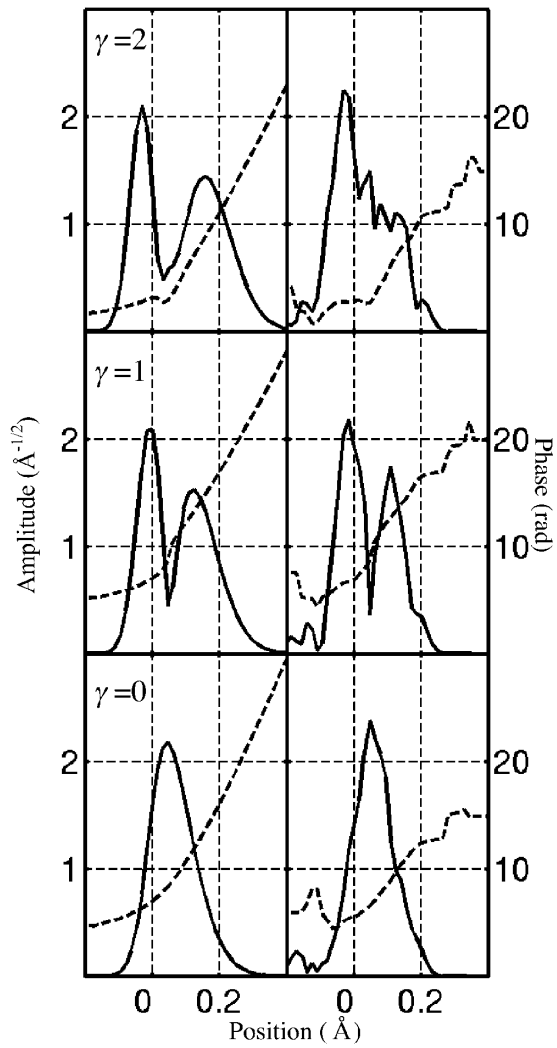

FIG. 3. Left: Amplitude (solid line) and phase (dashed line) of target wave packets prepared from a mixed initial state by a transform-limited pulse. Right: Same for wave packets reconstructed from the noisy signal.

prepared in adaptive laser control experiments, while requiring only rudimentary information about the electronic potential energy surface on which the photochemistry occurs. Although similar in spirit to linear QSH, state reconstruction by nonlinear WPI possesses a number of advantages. QSH detects the overlap between a one-pulse target wave packet and a one-pulse reference wave packet; the reference states all traverse a common phase-space path on the potential that also governs the target-state dynamics. In nonlinear WPI, the expanded collection of three-pulse reference states covers a higher-dimensional phase-space region. In addition, these reference states are prepared using known g and e states; if the Condon approximation applies (at least locally) and the preparation pulses are sufficiently brief, nonlinear WPI does not require detailed information about the f-state potential. Reconstruction of target wave packets could also provide direct information about the final-state potential-energy surface on which the target state propagates. By using targets reconstructed at multiple t_{43} delays and evaluation of $\partial\psi/\partial t$ by finite differencing, three-dimensional scans of the nonlinear WPI signal could be used to invert the Schrödinger equation and map the f-state potential in those regions sampled by the moving target wave packet [25].

This work was supported by the NSF and the J. S. Guggenheim Memorial Foundation. For helpful comments, we thank T. Dyke, G. R. Fleming, C. B. Harris, R. A. Harris, and A. H. Marcus.

*Electronic address: cina@uoregon.edu

[1] S. A. Rice and M. Zhao, *Optical Control of Molecular Dynamics* (Wiley, New York, 2000).
[2] T. Brixner, N. H. Damrauer, P. Niklaus, and G. Gerber, Nature (London) **414**, 57 (2001).
[3] J. L. Herek, W. Wohlleben, R. J. Cogdell, D. Zeidler, and M. Motzkus, Nature (London) **417**, 533 (2002).
[4] R. J. Levis, G. M. Menkir, and H. Rabitz, Science **292**, 709 (2001).
[5] T. J. Dunn, I. A. Walmsley, and S. Mukamel, Phys. Rev. Lett. **74**, 884 (1995).
[6] E. Skovsen, H. Stapelfeldt, S. Juhl, and K. Mølmer, Phys. Rev. Lett. **91**, 090406 (2003).
[7] C. Leichtle, W. P. Schleich, I. Sh. Averbukh, and M. Shapiro, Phys. Rev. Lett. **80**, 1418 (1998); I. Sh. Averbukh, M. Shapiro, C. Leichtle, and W. P. Schleich, Phys. Rev. A **59**, 2163 (1999).
[8] T. Weinacht, J. Ahn, and P. H. Bucksbaum, Nature (London) **397**, 233 (1999).
[9] J. A. Cina, J. Chem. Phys. **113**, 9488 (2000).
[10] N. F. Scherer, R. Carlson, A. Matro, M. Du, A. J. Ruggiero, V. Romero-Rochin, J. A. Cina, G. R. Fleming, and S. A. Rice, J. Chem. Phys. **95**, 1487 (1991); N. F. Scherer, A. Matro, R. J. Carlson, M. Du, L. D. Ziegler, J. A. Cina, and G. R. Fleming, J. Chem. Phys. **96**, 4180 (1992).
[11] K. Ohmori, Y. Sato, E. E. Nikitin, and S. A. Rice, Phys. Rev. Lett. **91**, 243003 (2003).
[12] M. Cho, N. F. Scherer, G. Fleming, and S. Mukamel, J. Chem. Phys. **96**, 5618 (1992).
[13] W. P. de Boeij, M. S. Pshenichnikov, and D. A. Wiersma, Chem. Phys. **233**, 287 (1998).
[14] J. D. Hybl, A. Albrecht Ferro, and D. M. Jonas, J. Chem. Phys. **115**, 6606 (2001).
[15] The absence of spectral amplitude at $\omega_{f\leftarrow e}$ makes bilinear terms negligible.
[16] P. Tian, D. Keusters, Y. Suzkai, and W. S. Warren, Science **300**, 1553 (2003).
[17] For the mth choice of (t_{21}, t_{32}) let $z_m = \langle \mathrm{ref}_{421,m}|\mathrm{tar}_3\rangle$. A set of M overlaps can be cast as $\mathbf{z} = \mathbf{R}\,\mathbf{t}$, where a discrete position basis of N points defines components of the unknown target vector, $t_n = \langle x_n|\mathrm{tar}_3\rangle$, and the $M \times N$ reference matrix, $R_{mn} = \langle \mathrm{ref}_{421,m}|x_n\rangle$.
[18] SVD decomposes the reference matrix as $\mathbf{R} = \mathbf{U}\mathbf{W}\mathbf{V}^\dagger$, with $\mathbf{U}$ an $M \times N$ matrix with orthonormal columns, $\mathbf{W}$ an $N \times N$ diagonal matrix with singular values $W_{nn} \geq 0$, and $\mathbf{V}$ an $N \times N$ unitary matrix. The reconstructed vector $\mathbf{r} = \mathbf{V}\mathbf{W}_\mathbf{M}^{-1}\mathbf{U}^\dagger\mathbf{z}$ minimizes the norm and residual, and is characterized by a fidelity $f = |\mathbf{t}^* \cdot \mathbf{r}|/(\|\mathbf{t}\| \cdot \|\mathbf{r}\|)$ lying between 0 and 1. In general, one makes use of the modified inverse, $\mathbf{W}_\mathbf{M}^{-1}$, which replaces the inverse of those singular values below some fractional cutoff (the tolerance T) with zero. See L. N. Trefethen and D. Bau, *Numerical Linear Algebra* (SIAM, Philadelphia, 1997).
[19] None of the specific features of this generic model are essential for successful state reconstruction.
[20] Primed quantities are chirp dependent; by equating power spectra for chirped and unchirped fields, primed parameters are related to their transform-limited values: $E_j' = E_j(\sigma_j'/\sigma_j)^{1/2}$ and $\sigma_j' = \sigma_j(1 + \delta_j^2/\sigma_j^4)^{1/2}$. The spectral phase $\phi_j(\omega) = \Phi_j + \tan^{-1}[\delta_j/\sigma_j^2] - \delta_j(\omega - \Omega_j)^2/2$ has linear frequency chirp δ_j related to the temporal chirp by $c_j = \delta_j/(\sigma_j^4 + \delta_j^2)$. Pulses 1, 2, and 4 are transform-limited with $\sigma_j = 3$ fs (intensity FWHM 5.00 fs). The third pulse is either transform-limited with $\sigma_3 = 12$ fs (FWHM 19.98 fs) or has a (maximal) temporal chirp $c_3 = \pm 1/2\sigma_3^2$, so that $\sigma_3' = \sqrt{2}\sigma_3 = 16.97$ fs. We select $\Omega_1 = \Omega_2 = \omega_L = \varepsilon_e + m\omega^2 x_e^2/2$ and $\Omega_3 = \Omega_4 = \omega_L' = \varepsilon_f + D$.
[21] C. Leforestier *et al.*, J. Comput. Phys. **94**, 59 (1991). We used a 0.05 fs time step and a 128-point position grid from -0.5 to 1.5 Å.
[22] T. S. Humble and J. A. Cina, Bull. Korean Chem. Soc. **24**, 1111 (2003) found unit fidelity in a noise-free one-color reconstruction. See also S. Ramos-Sánchez and V. Romero-Rochín, J. Chem. Phys. (to be published).
[23] In the short-pulse limit $P_4^{fg} \cong i(a_4\mu_{fg}/2)\exp(-i\Phi_4)$, where a_4 is the area under the pulse envelope, and construction of the reference matrix requires no detailed information about H_f.
[24] The $M \times \Gamma N$ reference matrix has elements $R_{ml} = w_\gamma\langle \mathrm{ref}_{421,m}^\gamma|x_n\rangle$, where Γ is the number of populated levels and the column index $l = n + \gamma N$. The target vector contains Γ wave packets in the position basis: $t_l = \langle x_n|\mathrm{tar}_3^\gamma\rangle$ with row index l.
[25] N. Dickson, T. S. Humble, and J. A. Cina (unpublished).